NASA

Technical Memorandum 86088

LARGE-SCALE INTERPLANETARY MAGNETIC FIELDS: VOYAGER 1 AND 2 OBSERVATIONS BETWEEN 1 AU AND 9.5 AU

L. F. Burlaga
L. W. Klein
R. P. Lepping
K. W. Behannon

APRIL 1984

National Aeronautics and
Space Administration

Goddard Space Flight Center
Greenbelt, Maryland 20771

Large-Scale Interplanetary Magnetic Fields: Voyager 1 and 2 Observations between 1 AU and 9.5 AU

by

L. F. Burlaga
NASA/Goddard Space Flight Center
Laboratory for Extraterrestrial Physics
Greenbelt, MD 20771

L. W. Klein
Applied Research Corporation
8201 Corporate Drive
Landover, MD 20785

R. P. Lepping
K. W. Behannon
NASA/Goddard Space Flight Center
Laboratory for Extraterrestrial Physics
Greenbelt, MD 20771

ABSTRACT

The strength B of the interplanetary magnetic field observed by the Voyager spacecraft between 1 AU and ∿ 9.5 AU was found to decrease with distance R from the sun as $B = 4.75\ (1 + R^2)^{1/2}/R^2$, in agreement with the spiral field model. Between August, 1977 and July, 1979, when solar activity was increasing, corotating flows were observed at an average rate of at least 1 every 20 days, but the flows were evolving with time and seldom recurred from one solar rotation to the next without change. Many transient flows were also observed in this period. Large-scale fluctuations in B with respect to the average spiral field were observed in association with interplanetary shocks and corotating stream interfaces, and these fluctuations varied with time in association with changes of the flows. The amplitude of the fluctuations in B relative to the mean field was large. There was a tendency for it to increase with distance to 5 AU, but the temporal variations were comparable to or larger than the radial variations. At large distances, B and the plasma density increased together, consistent with the idea that the structure of the outer heliosphere may be determined by stream interactions. The width of interaction regions increased with R owing to expansion, and closely spaced interaction regions often coalesced. A 4-sector pattern was observed from day 267, 1977, to approximately day 173, 1978, followed by a 2-sector pattern which lasted to at least day 179, 1979. In the interval with 4 sectors, there were usually several small-amplitude peaks in B together with many transient streams and shocks on each solar rotation, whereas in the interval with 2 sectors there were 1 or 2 maxima in B together with interfaces and shock pairs on each solar rotation. Thus, the relatively abrupt change in sector pattern was accompanied by a change in the pattern of fluctuations in B and a change in the nature of the dominant flows.

1. Introduction

The purpose of this paper is to describe the large-scale radial and temporal variations of the interplanetary magnetic field observed by Voyagers 1 and 2 between 1 AU and 9.5 AU. The magnetic field and plasma experiments on these spacecraft have been described by Behannon et al. (1977) and Bridge et al. (1977), respectively. The emphasis of our analysis is on the strength of the magnetic field, $|\underset{\sim}{B}| \equiv B$, but observations of the sector structure are presented in Section 4 and observations of interfaces and shocks are presented in Section 5, because these are important for understanding the variations of $|\underset{\sim}{B}|$. We consider the magnetic field strength B as the sum of two components, B_o and δB, where $B_o \equiv \langle |\underset{\sim}{B}| \rangle$ is the mean field computed by averaging over approximately a solar rotation and δB represents the large-scale fluctuations in B with respect to the mean field. Specifically, $\delta B = \bar{B} - B_p$, where $\bar{B}$ is a 10-hour or 24-hour average of B at a given time, and B_p is the value of the mean field, at the given time and position, derived from a best fit of B_o versus R to the theoretical curve given by the spiral field model of Parker (1958, 1963); here R is the radial distance from the sun.

Early studies of the radial variations of the interplanetary magnetic field were reviewed by Behannon (1978). Voyager observations of B(R) between 1 AU and 5 AU have been discussed by Burlaga et al. (1982). This paper extends that analysis to $\sim$ 9.5 AU, and it complements the studies based on Pioneer 10 and 11 observations made beyond 1 AU during a different part of the solar cycle (Smith, 1974 and 1979; Smith and Wolfe, 1979 and 1977; and Rosenberg et al., 1978). These early measurements indicated that the large scale field could be described by Parker's spiral field model (Parker, 1963), which gives

$$B_o = B_p(R) = A(1 + R^2)^{1/2}/R^2. \qquad (1)$$

Recently, however, Smith and Barnes (1983) reported that fields measured in the outer heliosphere by Pioneer 10 and 11 are weaker than expected on the basis of the spiral model. In Section 2 we show that no such systematic departures from the spiral model are found in the Voyager data.

The fluctuations of $|\underset{\sim}{B}|$ are studied by considering short term (10-hour or 24-hour) averages of B normalized with respect to the best-fit spiral field, i.e., we consider

$$\begin{aligned} \delta B/B_p &= \langle (B - B_p)/B_p \rangle \\ &= \langle B/B_p - 1 \rangle \end{aligned} \qquad (2)$$

or simply $\langle B/B_p \rangle$.

The statistical properties and temporal pattern of $\bar{B}/B_p$ are described in Section 3. We relate these large-scale fluctuations to the sector pattern in Section 4, and to dynamical processes associated with shocks and corotating streams in Section 5.

2. Magnetic Field Strength Versus Distance

To describe the radial variation of the magnetic field strength, it is appropriate to average over successive solar rotations. At a fixed point in space, the rotation period is close to 25 days, but it may vary depending on the solar latitude of the source of the solar wind. The radial variation of 25 day averages of $|\underset{\sim}{B}|$ for Voyager 1 and Voyager 2 is shown in Figure 1 and Figure 2, respectively. The Voyager 2 data extend from 1 AU (August 20, 1977) to 9.5 AU (August 10, 1981), and the Voyager 1 data extend from 1 AU (September 5, 1977) to 8.2 AU (July 1, 1980). For each averaging interval, we used hour averages of B to compute both the average $\langle |\underset{\sim}{B}| \rangle$ and a measure of the uncertainty of the average σ = RMS $/\sqrt{N}$, where N is the number of points in the average and RMS is the root-mean-square deviation of $|\underset{\sim}{B}|$. Each bar in Figures 1 and 2 has length equal to 2σ, and its center corresponds to $\langle |\underset{\sim}{B}| \rangle$. Each bar is plotted at a distance R equal to the average distance of the spacecraft in the averaging interval.

The points were fitted to the Parker spiral field model (1), by choosing the value A that gave minimum variance between the observations and the theoretical curve. For both the Voyager 1 and Voyager 2 data sets, we found A = 4.75. Inspection of Figures 1 and 2 show that the simple spiral field model gives a satisfactory zeroth order description of the radial variations of

interplanetary magnetic field strength. Smith and Barnes (1983) reported that, relative to observations made at 1 AU, the magnetic field strength observed by Pioneers 10 and 11 was significantly lower than that predicted by $B_p(R)$. In particular, the field strength observed out to $\sim$ 10 AU from 1977-1981 was significantly lower than that observed at 1 AU when adjusted by the factor $(1 + R^2)^{1/2}/R^2$. Slavin et al. (1983) found that the azimuthal component of the field decreases with distance from the sun as $R^{-1.12 \pm 0.04}$ using ISEE-3 and Pioneer 10, 11 data and as $R^{-1.27 \pm 0.06}$ using Helios and Pioneer data. This is significantly different from the R^{-1} dependence predicted by Parker's model, but similar behavior has been noted in previous studies (see Behannon, 1978).

We compared Voyager observations with those of IMP-8 and ISEE-3 at 1 AU, as given in the OMNI tape of King (private communication), in order that our results might be related more directly to those of Smith and Barnes (1983). The results are given in Figure 3, which shows 26 day averages of the magnetic field divided by $B_p(R) = 4.75\ (1 + R^2)^{1/2}/R^2$. For the 1 AU data, this normalization consists in simply dividing the observed field by the average field at 1 AU, $B_{p1} = 6.7$ nT. The normalized 1 AU data are shown by the light lines in Figure 3. Note that throughout 1980 the data scatter about the line $B/B_p = 1$ as expected for a quasi-stationary model. The Voyager 1 and 2 values of $< |\underset{\sim}{B}| >/B_p$ are shown at the bottom and top of Figure 3, respectively, by heavy lines. Because the solar wind propagation time from earth to Voyager can exceed 1 solar rotation period at large spacecraft distances ($\gtrsim$ 8 AU), the Voyager averages are shown at the time the wind would have passed 1 AU, assuming a constant radial propagation speed of 400 km/s. Comparing the Voyager observations of B/B_p with those made at 1 AU, we see no significant systematic difference. In particular, there is no evidence that the field observed by Voyagers 1 and 2 at large distances (large times) was significantly lower, relative to the observations made at 1 AU, than that predicted from (1).

3. Variability of the Large-scale Magnetic Field Strength

Having shown that the average magnetic field strength, $B_o(R)$, is given reasonably well by the spiral field model, $B_p(R)$, let us now consider the

fluctuations of B about this value. Figure 3 showed that there are at times large deviations from the spiral model even though the long-term agreement is good. As indicated in Section 1, equation (2), we studied the fluctuations of B by considering variations of $\langle B/B_p \rangle$. Since we are interested in relatively long-term fluctuations, we consider 10-hour averages of the ratio B/B_p. These "fluctuations" correspond to changes associated with individual flows, and at higher resolution they might be seen as ordered structures which could be described by deterministic models.

Figure 4 shows $\langle B/B_p \rangle$, which we shall write simply B/B_p, as a function of time for three 170-day intervals corresponding to three distance ranges of Voyager 1 viz. (1.0 to 2.6) AU, (4.0 to 5.2) AU and (6.9 to 8.2) AU. Several important characteristics of large-scale fluctuations of B can be seen in this figure. First, the fluctuations with respect to the mean field $B_p(R)$ can be large at all distances between 1 AU and 8 AU. Values of $B/B_p > 2$ are not uncommon, and values of $B/B_p > 1.5$ occur frequently. Thus, the fluctuations are not small amplitude disturbances; they represent non-linear effects. Second, Figure 4 suggests that the root-mean-square deviation (RMS) of the fluctuations does not change drastically with distance. This will be discussed in more detail below. Finally, one sees that the characteristic time scale (hence radial extent) of the fluctuations appears to increase with distance. Near 1 AU, the peaks in B/B_p are narrower and more closely spaced than at large distances. This figure alone does not allow us to rule out the possibility that the effect is due to long-term temporal fluctuations as the spacecraft moved from 1 AU to 8 AU. However, Burlaga and Goldstein (1984), using simultaneous data from 1 AU and (4-5) AU, showed that under some circumstances the ratio of energy at long wavelengths to that at small wavelengths does increase with distance from the sun.

Consider the RMS of $B/B_p(t)$ for the profiles shown in Figure 4. If the solar wind were stationary and composed of a series of identical streams, one might expect the RMS to first increase with R as the corotating pressure waves increase in amplitude due to kinematic steepening of the streams. However, one then expects a decrease in the RMS at large R where the pressure waves are no longer driver by the streams and free to expand, if the streams are isolated from one another. Figure 5 shows a plot of the RMS of B/B_p versus R

for Voyager 1 and 2 data between 1 AU and ∿ 9 AU. Each point is an average of RMS (B/B_p) over an interval of 100 days. Figure 5 shows a tendency for the RMS to increase with R out to ∿ 6 AU, but the fluctuations in the RMS are large and a simple variation of the type expected for stationary flows is not observed. Clearly temporal variations are important. The figure implies that if we wish to understand the radial variation of the fluctuations of B/B_p, we must separate temporal from spatial effects, and we must better understand the nature of the fluctuations. Figure 5 shows that the average RMS of B/B_p between 1 AU and 9 AU is approximately 0.7, demonstrating that the fluctuations in B about the values given by the spiral field model are typically large.

Another way of looking at the fluctuations of B/B_p as a function of distance is to plot distributions of B/B_p for several distance intervals. Figure 6 shows distributions of log (B/B_p) for 10-hour averages of B/B_p at 4 distance intervals, (1 to 2) AU, (3 to 4) AU, (5 to 6) AU and (7 to 8) AU. At 1 to 2 AU one sees a relatively narrow distribution similar to the gaussian distribution which is generally seen at 1 AU (Burlaga and King, 1979; Slavin, 1983). Deviations from a gaussian with a peak at $B/B_p = 1$ can be attributed to statistical fluctuations in our sample, since the number of points N_o in the distribution is relatively small (N_o ∿ 300). At large distances, from 5 to 6 AU and from 7 to 8 AU, the distributions are broader and more irregular, presumably reflecting the dynamical process associated with the radial evolution of the flows. Moreover, the distributions observed by Voyager 1 in a given distance interval differ from those observed by Voyager 2 in the same distance interval, indicating again that temporal variations are important.

To provide an overview of the fluctuations in B as a function of time for the entire interval during which Voyagers 1 and 2 moved from 1 AU to ∿ 9 AU, we show daily averages of B/B_p from Voyager 2 data plotted in successive 27 day intervals arranged vertically in Figure 7. A 24-hour average of B/B_p tends to reduce the amplitude of the individual peaks and to merge peaks separated by less than 1 day, but the basic features that we wish to discern (the number and locations of the major peaks in B/B_p) are clearly shown. The pattern is complex, but two features are particularly significant. The pattern is not stationary, for it does not exactly repeat itself with a period

close to the solar rotation period. In fact, there are few times when the profile of $B/B_p(t)$ in one 27-day interval is similar to that in the next 27-day interval, in this particular epoch of the solar cycle. This implies that any stationary flow model must be applied with caution, particularly when considering intervals longer than 1 solar rotation.

A second significant feature of the pattern in Figure 7 is that at large distances and later times there are typically 1 or 2 large maxima in $B/B_p(t)$ per 27-day interval, whereas at smaller distances and early times one typically sees many smaller maxima. This was also implied by the data in Figure 4. The formation of a few large maxima at larger distances may be the result of entrainment of slow streams and interaction regions by faster moving streams, as discussed by Burlaga et al. (1983), but it may also be due in part to a change in the nature of the flows coming from the sun at later times. For example at early times the flows may be predominantly transient, whereas at later times a few large corotating streams might be dominant.

To fully understand the pattern in Figure 7 it will be necessary to study the individual interaction regions and flows, their dynamical evolution with increasing R, and their relation to the sun. This is a major task which we shall not undertake in this paper. Another approach is suggested by the observation that magnetic field strength enhancements are associated with sector boundaries (see, e.g., Behannon, 1976), and from the results of Burlaga and King (1979) that a maximum in B(t) at 1 AU is usually associated with either a shock or a corotating stream interface and occasionally associated with a "cold magnetic field strength enhancement" (Burlaga et al., 1978) such as a magnetic cloud (Burlaga et al., 1981). Thus, in the next two sections we discuss the sector pattern, the pattern of shocks and interfaces, and the relations between these patterns and that of B/B_p.

4. The Sector Pattern Observed by Voyagers 1 and 2

During the period of study the interplanetary magnetic field direction was highly variable, particularly in 1977 and early 1978, so that it was often difficult to identify the polarity in a short interval of say 8 hours or less. Furthermore, the data are not continuous; typically there is a gap of a few

hours each day, owing to a lack of tracking during that time. For these reasons we consider only the dominant polarity in a 24-hour interval, as determined from hour averages of $\underline{B}$. If less than 8 hours of data were available on a given day, no polarity was calculated. The field was assigned a positive polarity (+) corresponding to a field vector directed away from the sun if $\geq$ 2/3 of the measurements showed the field to be directed outward. Similarly, the field was assigned negative or mixed polarity, if > 2/3 of the measurements showed the field to be directed inward. The field was considered to be directed outward or inward if it was within 30° of the spiral field direction; otherwise the polarity is said to be "mixed" and is denoted by a dot.

The patterns of magnetic polarities observed by Voyagers 1 and 2 are shown in Figures 8 and 9, where each horizontal line shows a 27-day interval and successive 27-day intervals are plotted downward. The choice of 27 days is simply traditional; it does not necessarily represent the recurrence period of the solar wind observed by Voyager. However, the recurrence period should be close to 27 days, so this format is suited for displaying the basic sector pattern and its evolution with time. The line segments drawn in Figures 8 and 9 are meant to delineate the boundaries and individual sectors. In some cases the sector boundaries are clear, but in many cases they are not clear, either because of the presence of intervals with mixed polarities or because of data gaps. In the latter case, the line segments should be regarded as giving approximations to the sector structure, with an uncertainty which may be estimated by inspection of the figure.

The basic result in Figures 8 and 9 is that from day 268, 1977, to approximately day 173, 1978, 4-sectors were observed by Voyagers 1 and 2, while from 173, 1978 to 51, 1979 2 sectors were dominant. Essentially the same pattern was observed at 1 AU, as reported by Sheeley and Harvey (1979), so the Voyager sector pattern may be regarded as a mapping of the sector pattern at 1 AU. Small distortions of this pattern owing to latitudinal gradients and/or stream dynamics might be present, but they clearly do not alter the general pattern. The sector pattern is presumably established close to the sun. The inferred neutral lines for this period published by Hoeksema et al. (1983) are generally consistent with the interplanetary observations, but there are differences which merit further study.

There are many intervals in Figures 8 and 9 in which sectors are not clearly defined because of days with mixed polarity or days with 'foreign' polarity. This is particularly true during the 4-sector pattern. It is possible that this is due to the presence of transients. Their polarities may differ from that of the background flow and they may be ambiguous if the convected magnetic fields are at large angles with respect to the ecliptic. Mixed magnetic polarities might also indicate that the heliospheric current sheet is nearly parallel to the ecliptic, as discussed by Behannon and Burlaga (1983).

The relation between large-scale fluctuations in magnetic field strength B/B_p and the sector structure for the Voyager 2 data may be seen by comparing Figures 7 and 9. The same relation for the Voyager 1 data is shown on the left of Figure 10, where the sector structure from Figure 8 is superimposed on a plot of B/B_p computed from Voyager 1 data. The change from a 4-sector pattern to a 2-sector pattern was accompanied by a change in the B/B_p pattern. In the interval with 4 sectors, there were several small amplitude peaks in B/B_p on each solar rotation, whereas in the interval with 2 sectors there were one or two large peaks in B/B_p on each solar rotation. Since the change in the B/B_p pattern is relatively abrupt and related to a similarly abrupt change in the sector pattern, it is possible that it is caused primarily by a change in the nature of the flows, rather than simply a radial dependence of B/B_p and the stream structure. Daily averages of the bulk speed observed by Voyager 1 are shown together with the sector pattern from Figure 8 on the right of Figure 10. There tends to be one stream in each sector, with 1 or 2 large streams per solar rotation when the 2-sector pattern structure was observed and 3 or 4 small streams per solar rotation when the 4-sector pattern was observed. This is only a tendency, not a rule, and the association between streams and sectors is relatively weak in the interval with 4 sectors per solar rotation.

Studies based on 1 AU data have shown that maxima in the strength of the magnetic field are observed within a day following sector boundaries, at least under circumstances when the sector structure is well-defined. Well-defined sector boundaries were identified from among all those indicated in Figure 9

by requiring that there be a well-determined polarity for at least two days before the boundary and the opposite polarity for at least two days following the boundary. The times of these sector boundaries are indicated by the X's in Figure 7, so that they can be compared directly with the Voyager 2 observations of B/B_p. One does not find a simple relation between sector boundaries and maxima in B/B_p. Several of the sector boundaries were not associated with distinct maxima in B/B_p. In cases where the maxima in B/B_p occurred within 2 days of the sector boundaries, 33% occurred before the boundary and 44% occurred after the boundary. Forty-four percent of the crossings were preceded or followed by a peak in B/B_p within a day, and 77% were preceded or followed by a peak in B/B_p within 2 days. The probability of observing a peak in B/B_p by chance within ± 1 day (± 2 days) of a sector boundary for the sector pattern in Figure 9 is 0.23, (0.46). The observed probability of finding a maximum in B/B_p near a sector boundary is significantly higher than one might expect by chance, particularly when the 2-sector pattern was observed. Thus, the organization of B/B_p is related in some way to the sector pattern. However, the relation is not direct, and the physical reason for it cannot be derived from Figure 7.

5. Shocks, Interfaces and Magnetic Field Strength Enhancement

At 1 AU, peaks in magnetic field strength are associated with corotating interaction regions, shocks and some post-shock flows, and magnetic clouds. For example, Burlaga and King (1979) found that from 1963-1975, 52% of the enhancements occurred at stream interfaces in corotating interaction regions, 27% occurred behind shocks, and 11% occurred in cold regions not associated with shocks or interfaces. Thus, to interpret the pattern of magnetic field strength fluctuations, it is reasonable to examine its relation to the pattern of shocks and interfaces.

We have attempted to identify the shocks and interfaces observed from the launch of Voyagers 1 and 2 in 1977 to day 186 of 1979. The results are shown in Figures 11 and 12. Before drawing conclusions from these figures, we wish to stress the following limitations of the analysis. The shocks and interfaces were identified using hour averages of the plasma and magnetic field, and no detailed analysis of the discontinuities was made. A "forward

shock" was recognized as a discontinuous change in 27-day plots of hour averages, across which the density, N, field strength, B, proton temperature T, and bulk speed V increased simultaneously. A reverse shock was identified as a discontinuous decrease in N, T, B and increase in V. Non-linear waves which were in the process of steepening into shocks would thus be identified as shocks, even if they were not fully developed shocks. A stream interface was identified as an abrupt change characterized by a decrease in density, increase in temperature, and deflection in flow direction at which the magnetic field strength reaches a maximum, in accordance with the definition of Burlaga (1974). This definition is relatively unambiguous near 1 AU, but a stream interface might be difficult to observe at large distances, where fast corotating streams may have entrained slower streams, and the streams themselves have evolved appreciably. Finally, we stress that there were many data gaps, typically several hours each day, so that there were probably shocks and interfaces that are not identified in Figures 11 and 12. Moreover the identifications that were made might themselves be affected by data gaps, so they may be imperfect for this reason as well. Despite its limitations, our procedure for identifying shocks and interfaces is adequate to determine their general pattern in time. In Figures 11 and 12, forward shocks are denoted by solid vertical lines, reverse shocks by dashed vertical lines, and interfaces by solid dots.

In the second half of the interval shown in Figures 11 and 12, from 200, 1978, to 186, 1979, the pattern is dominated by corotating forward and reverse shocks with an interface in between. Earlier, most of the observed shocks were not associated with interfaces. Corotating shock pairs form beyond 1 AU, (Smith and Wolfe, 1976), so one expects them to become more abundant with increasing distance. It is surprising, however, that the transition occurs rather abruptly on the rotation beginning on day 200, 1978. This is just when the 4-sector pattern was replaced by a 2-sector pattern (see Figures 8 and 9). It seems that there was a change in the character of the flows associated with a change in the sector pattern. The 2-sector interval tends to be dominated by corotating interaction regions while the 4-sector interval has many transient shocks. This is only a tendency, however, for many interfaces were observed in the 4-sector interval, and there were times in the 2-sector interval in which no interfaces were seen (e.g., days 51 to 105, 1979).

Figure 13a,b shows again the daily averages of B/B_p for Voyager 2, together with the times of shocks and interfaces from Figure 12. Figure 13a and Figure 13b show the times of the 4-sector pattern and that of the 2-sector pattern, respectively. Since we have probably not identified all the shocks and interfaces that were present, we cannot expect to explain all the maxima in B/B_p as related to shocks or interfaces. Nearly all of the interfaces occurred within one day of a maximum in B/B_p. In other words, an interface is generally accompanied by a peak in B/B_p, at large distances as well as near 1 AU, and in a 2-sector pattern as well as in a 4-sector pattern. This is expected, since an interface is a signature of an interaction region where fast plasma overtakes and compresses slower plasma and magnetic fields. It is significant that the amplitude of the peaks in B/B_p tends to increase with R out to 5 AU (day 13, 1979, for Voyager 2). Note that there is no evidence for relaxation of the corotating pressure waves out to this distance. The corotating forward and reverse shock pairs are all accompanied by an interface between them, so they are associated with a peak in B/B_p. Many of the largest fluctuations in B/B_p are related to such shock pairs, but a shock pair does not necessarily produce a large amplitude fluctuation. Forward shocks which occur a day or two ahead of an interface and reverse shocks which occur a day or two after an interface are probably corotating shocks. The remaining forward shocks are probably transients. These are associated with an increase in B, of course, but not necessary with a maximum in B. When they are followed by a maximum in B, the amplitude is not necessarily large. The time at which magnetic clouds were observed by Burlaga and Behannon (1982) are denoted by C, and some other events that are possibly magnetic clouds are denoted by C? Note that some of the largest fluctuations in B/B_p are associated with magnetic clouds.

We cannot relate every peak in B/B_p to a shock, interface or magnetic cloud, but that may be due, at least in part, to the fact that we cannot identify all of these features that might be present. However, Figure 13 shows that in most cases ($\gtrsim$ 75%) the two largest peaks in B/B_p on a given solar rotation are associated with shocks, interfaces or magnetic clouds. We conclude that most of the large fluctuations in B/B_p in the region between 1 AU and 5 AU are associated with either the compression produced by shocks,

stream-steepening and entrainment or with magnetic flux carried from the sun by magnetic clouds and post-shock flows. This situation is similar to that at 1 AU. Probably the most significant difference is the apparent growth in amplitude and spatial extent of the fluctuations associated with interfaces. The increase in amplitude may be due both to the kinematic steepening of isolated streams and to the entrainment of slower moving flows including shocks and magnetic clouds. The relative importance of these two processes is not yet clear.

The increase in width of the magnetic field strength enhancements associated with shock pairs as a function of radial distance is due to the motion of the forward and reverse shocks away from the interface between them. Figure 14 shows the observed time Δt between the forward and reverse shock of a given pair as a function of the radial distance at which they were observed. Results from both Voyager 1 and Voyager 2 are shown. The tendency for Δt to increase with R is shown very clearly. From the slope of the line drawn through the points in Figure 14 one can derive a lower limit on the relative speed V_R between the forward and reverse shocks. Assuming that $\Delta t \backsim L/V_{SW}$, where L is the distance between the shocks at a given R and V_{SW} = 400 km/s, the speed with which the shocks are convected away from the sun, and setting $L \backsim V_R \times t$ where $t \backsim R/V_{SW}$, one obtains $V_R \backsim V_{SW}^2 (\Delta t/R) \backsim 90$ km/s. This is a lower limit, because the shocks form somewhere beyond 1 AU, rather than at R = 0. It is significant that this lower limit is close to twice the Alfvén speed. If we assume that most of the shocks formed at 3 to 4 AU, as Figure 14 suggests, the relative shock speed is approximately 180 to 270 km/s.

If the large fluctuations in B/B_p were produced by compression, either by shocks or by streams, then one should expect that B/B_p should increase with N/N_o. Some evidence that this is so has been presented by Burlaga (1983). This relation is shown as a function of distance in Figure 15. Near 1 AU, the fluctuations in B/B_p observed by Voyager 1 were small, and no correlation with density was observed. Beyond 4 AU, a significant correlation between B and N was observed, which is consistent with the idea that the large amplitude fluctuations in B/B_p observed in the second half of 1978 and early 1979 (Figure 13b) were produced by stream steepening and entrainment.

6. Summary and Discussion

The radial variation of the interplanetary magnetic field strength B observed by Voyagers 1 and 2 between 1 AU and ∿ 9.5 AU has been described. Two components of the magnetic field strength were considered in the study: an average component, B_o, based on solar rotation averages, and a fluctuation component δB, expressed by 10 or 24-hour averages of B normalized by the best-fit average field for the corresponding time and distance.

The radial variation of the average component, B(R) was consistent with the predictions of Parker's spiral field model, $B(R) = A(1 + R^2)^{1/2}/R^2$. For both Voyager 1 and Voyager 2 data, a least squares fit of the observations to Parker's curve gave A = 4.75. No evidence for systematic deviations from Parker's model was observed. In particular, there is no statistically significant evidence of a tendency for the field strength to decrease more rapidly than the spiral field model predicts. Large scatter about the best fit curve was observed, even when solar rotation averages of the field strength were plotted. This is presumably related to particular flow variations; the solar wind is not stationary as assumed in the spiral field model.

The large-scale fluctuations in B about the spiral field curve formed a relatively complex pattern, but it was not without order. Enhancements in B/B_p tended to be broader at larger distances, possibly due in part to expansion of individual pressure waves and interaction of distinct pressure waves. The amplitude of the large-scale fluctuations tended to increase with distance out to ∿ 5 AU, but temporal variations were evidently nearly as important as radial variations in determining the amplitude of B/B_p. Recurrent patterns with a fixed period of say 25-28 days were not observed and the pattern generally changed to some extent from one solar rotation to the next. The distributions of B/B_p were generally less "gaussian", broader, and more irregular at larger distances. In some cases, different distributions were observed by Voyager 1 and 2 in the same range of radial distances, presumably because the two spacecraft moved through the regions at different times. This again indicates the importance of temporal variations and the difficulty of separating spatial and temporal variations.

The variability of B was closely related to the variability of the interplanetary flows. Many transient streams and shocks were observed, particularly in the second half of 1978 and the first half of 1979. Corotating streams were also abundant, occurring at a rate of at least one every 20 days on average, although the distribution in time was not uniform. These corotating streams, observed at a time when solar activity was increasing, were not stationary. They often changed significantly from one solar rotation to the next, with differences in the speed profile and magnetic field strength profile. The recurrence time was variable, and in many instances corotating streams did not recur at all. Burlaga et al. (1978) have previously shown that corotating streams and even recurrent streams may be non-stationary, and Pizzo (1983) has discussed this from a theoretical point of view.

A 4-sector pattern was observed by Voyagers 1 and 2 from day 268, 1977, to $\sim$ 173, 1978, and a 2-sector was observed thereafter until approximately day 173 of 1979. This abrupt change in sector structure was related to a change in the general pattern of large-scale fluctuations in B/B_p. In the interval with 4 sectors, there were several small amplitude peaks in B/B_p on each solar rotation, whereas in the interval with 2 sectors there were 1 or 2 large peaks in B/B_p on each solar rotation. 77% of the well-defined sector boundary crossings were associated with a maximum in B/B_p within ± 2 days of the boundary; 44% of these maxima in B/B_p occurred after the boundary and 33% before the boundary. 44% of the boundaries were associated with a peak in B/B_p within ± 1 day of the boundary.

The pattern of shocks and interfaces observed by Voyagers 1 and 2 was determined to the extent that limitations due to gaps in data coverage and the use of the hour averages allowed. In the interval with 4 sectors, there were many forward shocks which were not accompanied by interfaces, whereas in the interval with 2 sectors corotating forward and reverse shocks were a dominant feature. Evidently, the character of the flows changed when the sector pattern changed. The situation was complex in detail, however, for there were times in the 2-sector interval when no interfaces were seen, and many interfaces were observed in the 4-sector interval. Nearly all of the

interfaces were associated with maxima in B/B_p, as expected. The peaks in B/B_p associated with interfaces were generally higher and broader at larger distances, particularly in the interval with 2 sectors per solar rotation. The value of B/B_p increased behind shocks, as expected, but shocks were not always followed by a distinct maximum in B/B_p. Some of the largest maxima in B/B_p were associated not with shocks or interfaces but with magnetic clouds. Many of the largest fluctuations in B/B_p were related to shock pairs, but a shock pair did not always produce a large enhancement in B/B_p. The observed separation between shocks increased with distance, at a rate consistent with an average relative shock speed of 200 to 300 km/sec if most shocks form at 3 or 4 AU. Most, and possibly all of the large peaks in B/B_p were associated with a shock, an interface or a magnetic cloud. At distances $\gtrsim$ 3 AU, B/B_p was well-correlated with N/N_p, indicating that there most of the enhancements were produced by compression in the interplanetary medium, e.g., by shocks, stream steepening or entrainment.

We have described above a number of the general features of the large-scale magnetic field pattern observed by the Voyager spacecraft, and we found some order, but the pattern was basically complex during this epoch. In particular, a basic conclusion is that temporal variations cannot be ignored; the flows were generally not stationary, even though many corotating streams were present. More detailed studies of individual flows, using data from several spacecraft are needed to separate spatial and temporal effects and to understand the basic dynamical processes involved. The present work allows one to view these detailed studies in the proper perspective. Additional statistical studies, such as that of Burlaga and Goldstein (1984) using data from at least two spacecraft, will also be instructive. But the present work shows that care must be taken in choosing samples to be studied, because the patterns are not always "stationary" and "homogeneous".

Acknowledgments

The magnetic field data for this study were provided by the Principal Investigator, N. Ness and the plasma data are from the MIT experiment Principal Investigator, H. Bridge. ISEE-3 magnetic field data from the experiment of E. Smith were provided by the NSSDC.

References

Behannon, K. W., Observations of the interplanetary magnetic field between 0.46 and 1 A. U. by the Mariner 10 spacecraft, Ph.D. Dissertation, Catholic University of America, 1976; also NASA/GSFC X-692-76-2, 1976.

Behannon, K. W., Heliocentric distance dependence of the interplanetary magnetic field, Rev. Geophys. Space Phys., 16, 125, 1978.

Behannon, K. W., M. H. Acuña, L. F. Burlaga, R. P. Lepping, N. F. Ness, and F. M. Neubauer, Magnetic field experiment for Voyagers 1 and 2, Space Sci. Rev., 21, 235, 1977.

Behannon, K. W., L. F. Burlaga, and A. J. Hundhausen, A comparison of interplanetary current sheet inclinations, J. Geophys. Res., 88, 7837, 1983.

Bridge, H. S., J. W. Belcher, R. J. Butler, A. J. Lazarus, A. M. Mavretic, J. D. Sullivan, G. L. Siscoe, and V. M. Vasyliunas, The plasma experiment on the 1977 Voyager mission, Space Sci. Rev., 21, 259, 1977.

Burlaga, L. F., Interplanetary stream interfaces, J. Geophys. Res., 79, 3717, 1974.

Burlaga, L. F., Corotating pressure waves without fast streams in the solar wind, J. Geophys. Res., 88, 6085, 1983.

Burlaga, L. F., and K. W. Behannon, Magnetic clouds between 2-4 AU, Solar Phys., 81, 181, 1982.

Burlaga, L. F., and M. L. Goldstein, Radial variations of large-scale magnetohydrodynamic fluctuations in the solar wind, submitted to J. Geophys. Res., 1984.

Burlaga, L. F., and J. King, Intense interplanetary magnetic fields observed by geocentric spacecraft during 1963-1975, J. Geophys. Res., 84, 6633, 1979.

Burlaga, L. F., N. F. Ness, F. Mariani, B. Bavassano, U. Villante, H. Rosenbauer, R. Schwenn, and J. Harvey, Magnetic fields and flows between 1 and 0.3 AU during the primary mission of Helios 1, J. Geophys. Res., 83, 5167, 1978.

Burlaga, L. F., R. P. Lepping, K. W. Behannon, L. W. Klein, and F. M. Neubauer, Large scale variations in the IMF: Voyager 1 and 2 observations between 1-5 AU, J. Geophys. Res., 87, 4345, 1982.

Burlaga, L., E. Sittler, F. Mariani, and R. Schwenn, Magnetic loop behind an interplanetary shock: Voyager, Helios and IMP-8 observations, J. Geophys. Res., 86, 6673, 1981.

Burlaga, L., R. Schwenn, and H. Rosenbauer, Dynamical evolution of interplanetary magnetic fields and flows between 0.3 AU and 8.5 AU: Entrainment, Geophys. Res. Lett., 10, 413, 1983.

Hoeksema, J., J. M. Wilcox, and P. H. Scherrer, The structure of the heliospheric current sheet: 1978-1982, J. Geophys. Res., 88, 9910, 1983.

Parker, E. N., Dynamics of the Interplanetary gas and magnetic fields, Astrophys. J., 128, 664, 1958.

Parker, E. N., Interplanetary dynamical processes, Interscience Publishers, New York, 1963.

Pizzo, V., Quasi-steady solar wind dynamics, Solar Wind Five, edited by Marcia Neugebauer, p. 675, NASA Conference Publication 2280, 1983.

Rosenberg, R. L., M. G. Kivelson, P. J. Coleman, Jr., and E. J. Smith, The radial dependences of the interplanetary magnetic field between 1.0 and 5.0 AU: Pioneer 10, J. Geophys. Res., 83, 4165, 1978.

Sheeley, N. R., Jr., and J. W. Harvey, Coronal holes, solar wind streams, and geomagnetic disturbances during 1978 and 1979, Solar Phys., 70, 237, 1981.

Slavin, J. A., E. J. Smith, and B. T. Thomas, Large scale temporal and radial gradients in the IMF: Helios 1, 2, ISEE-3, and Pioneer 10, 11, Geophys. Res. Lett., in press, 1983.

Smith, E. J., Radial gradients in the interplanetary magnetic field betwen 1.0 and 4.3 AU: Pioneer 10, in Solar Wind Three, edited by C. T. Russell, University of California Press, Los Angeles, 1974.

Smith, E. J., Interplanetary magnetic fields, Rev. Geophys. Space Phys., 17, 610, 1979.

Smith, E. J., and A. Barnes, Spatial dependences of the solar wind, 1-10 AU, in Solar Wind Five, edited by M. Neugebauer, p. 521, NASA Conference Publication 2280, 1983.

Smith, E. J., and J. H. Wolfe, Observations of interaction regions and corotating shocks between one and five AU: Pioneers 10 and 11, Geophys. Res. Lett., 3, 137, 1976.

Smith, E. J., and J. H. Wolfe, Fields and plasmas in the outer solar system, Space Sci. Rev., 23, 217, 1979.

Smith, E. J., and J. H. Wolfe, Pioneer 10, 11 observations of evolving solar wind streams and shocks beyond 1 AU, in Study of Traveling Interplanetary Phenomena, edited by M. A. Shea et al., pp. 227-257, D. Reidel, Hingham, Mass., 1977.

Figure Captions

FIGURE 1 — 25-day averages of the interplanetary magnetic field magnitude measured by Voyager 1 as a function of radial distance from the sun. The curve is the prediction of the spiral field model with the constant A = 4.75 determined from a least squares fit to the data.

FIGURE 2 — Same as Figure 1, except that Voyager 2 data are plotted.

FIGURE 3 — 26-day averages of B/B_p, where B_p is the field strength derived from the spiral model for a given t(R), as a function of time. Heavy lines are Voyager 1 and 2 data projected to 1 AU assuming a time delay appropriate for corotating flows with a constant solar wind speed of 400 km/s. The light line is the field strength observed at 1 AU, with B_p 6.7 nT; it was derived from IMP-8 and ISEE-3 data. No significant systematic differences are observed between the Voyager data obtained at large distances from the sun and the 1 AU data.

FIGURE 4 — Examples of the large-scale fluctuations in B/B_p observed by Voyager 1 at three different distances from the sun, 10-hour averages of B/B_p are plotted.

FIGURE 5 — The RMS of B/B_p computed for successive 100-day intervals, plotted as a function of radial distance from the sun. Each point is the average distance of the spacecraft in the corresponding 100-day interval.

FIGURE 6 — Distributions of 10-hour averages of B/B_p at different distances from Voyager 1 and 2 data.

FIGURE 7 — Daily averages of B/B_p determined from Voyager 2 data plotted in successive 27-day intervals. The X'S represent the positions of well-defined sector boundaries (see Figure 9).

FIGURE 8 The sector pattern observed by Voyager 1. + (-) denotes field lines directed toward (away from) the sun, and • denotes mixed polarity. Lines corresponding to sector boundaries are drawn to dilineate the general sector pattern, but note that in many cases the appropriate position of a line is uncertain.

FIGURE 9 Same as Figure 8, for Voyager 2 data.

FIGURE 10 Left: The sector pattern from Figure 8 superimposed on a plot of daily averages of B/B_p from Voyager 1 data. Right: The sector pattern from Figure 8 superimposed on a plot of daily averages of the bulk speed measured by Voyager 1.

FIGURE 11 This shows the temporal locations of forward shocks (solid lines) reverse shocks (dashed lines), interfaces (solid dots) and magnetic clouds (denoted by "C", identified using hour averages of plasma and magnetic field data from Voyager 1. Shaded areas indicate data gaps.

FIGURE 12 The same as Figure 11, except that the results are for Voyager 2.

FIGURE 13 Daily averages of B/B_p from Figure 7 together with the locations of shocks, interfaces and clouds from Figure 12, for both the 4-sector period (a)) and the 2-sector period (b).

FIGURE 14 The time interval between the arrival of a forward shock and a corresponding reverse shock for shock pairs identified by Voyager 1 and 2 plotted as a function of the distance at which the shock pair was observed.

FIGURE 15 B/B_p versus N/N_p, where N is the plasma density, and $N_p = 6\ (R(AU))^{-2}$ for six different distance intervals.

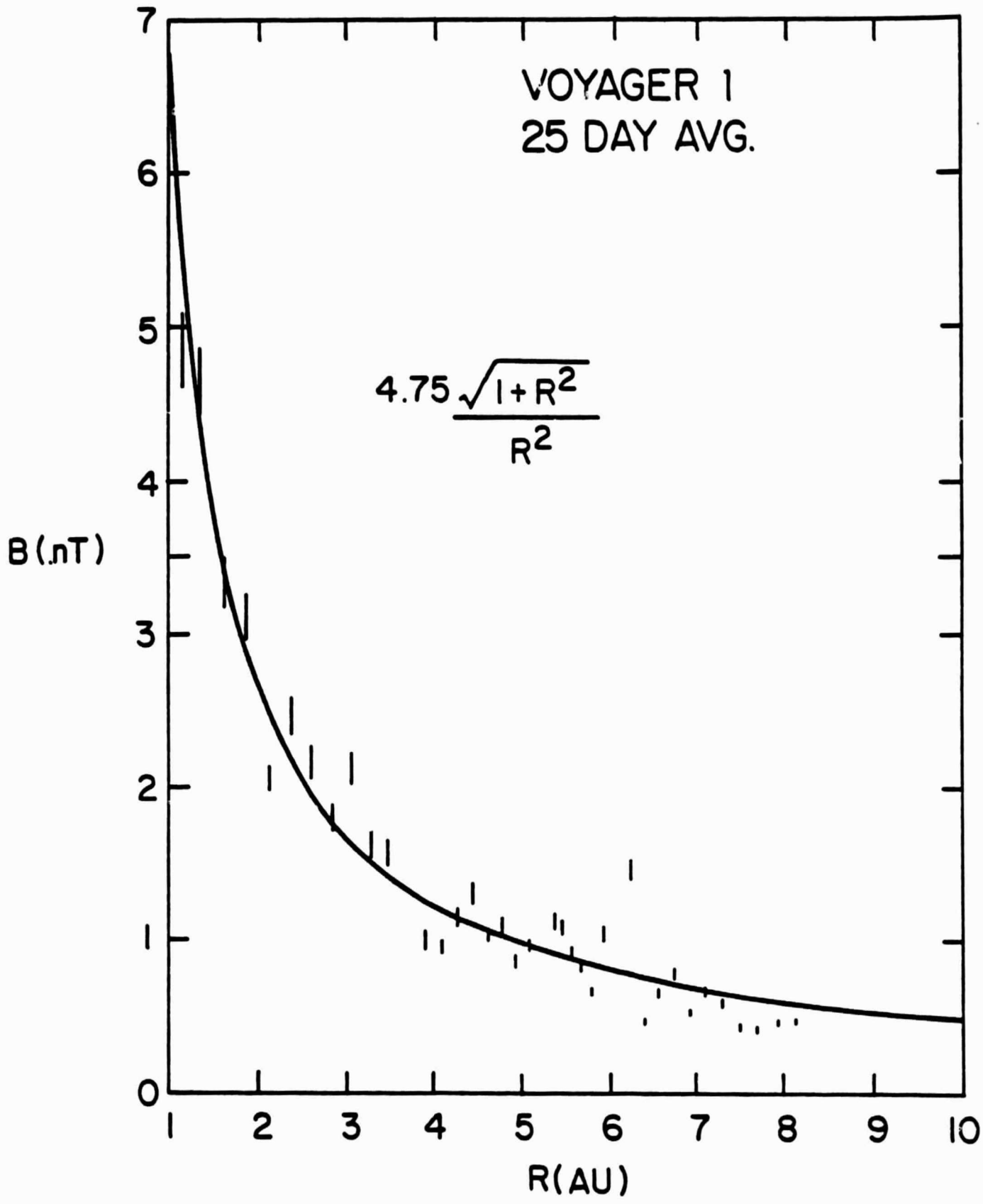
VOYAGER 1
25 DAY AVG.
$4.75\frac{\sqrt{1+R^2}}{R^2}$
B(nT)
R(AU)
0
1
2
3
4
5
6
7
8
9
10

Figure 1

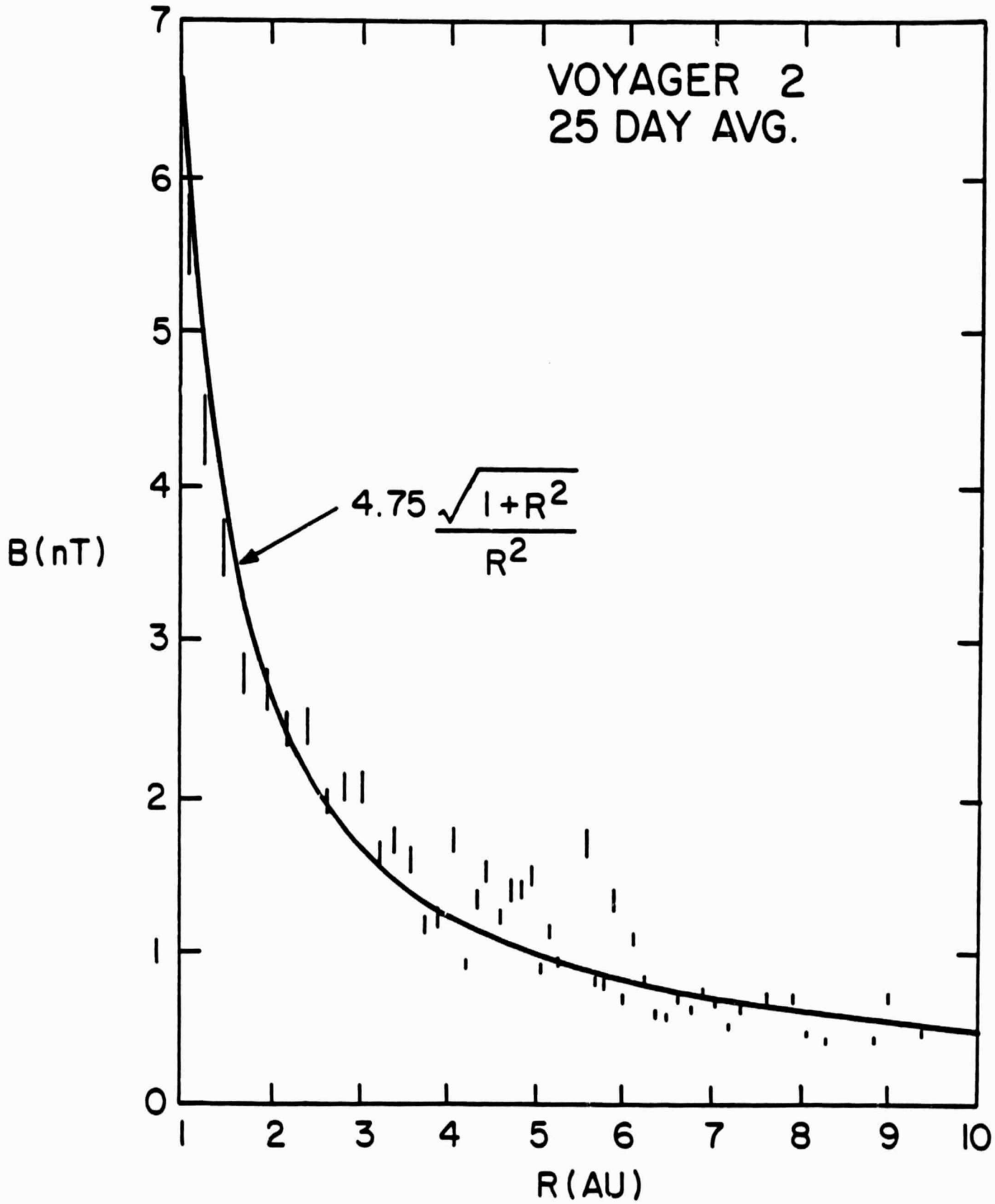
VOYAGER 2
25 DAY AVG.
$4.75\frac{\sqrt{1+R^2}}{R^2}$
B(nT)
R(AU)
0
1
2
3
4
5
6
7
8
9
10

Figure 2

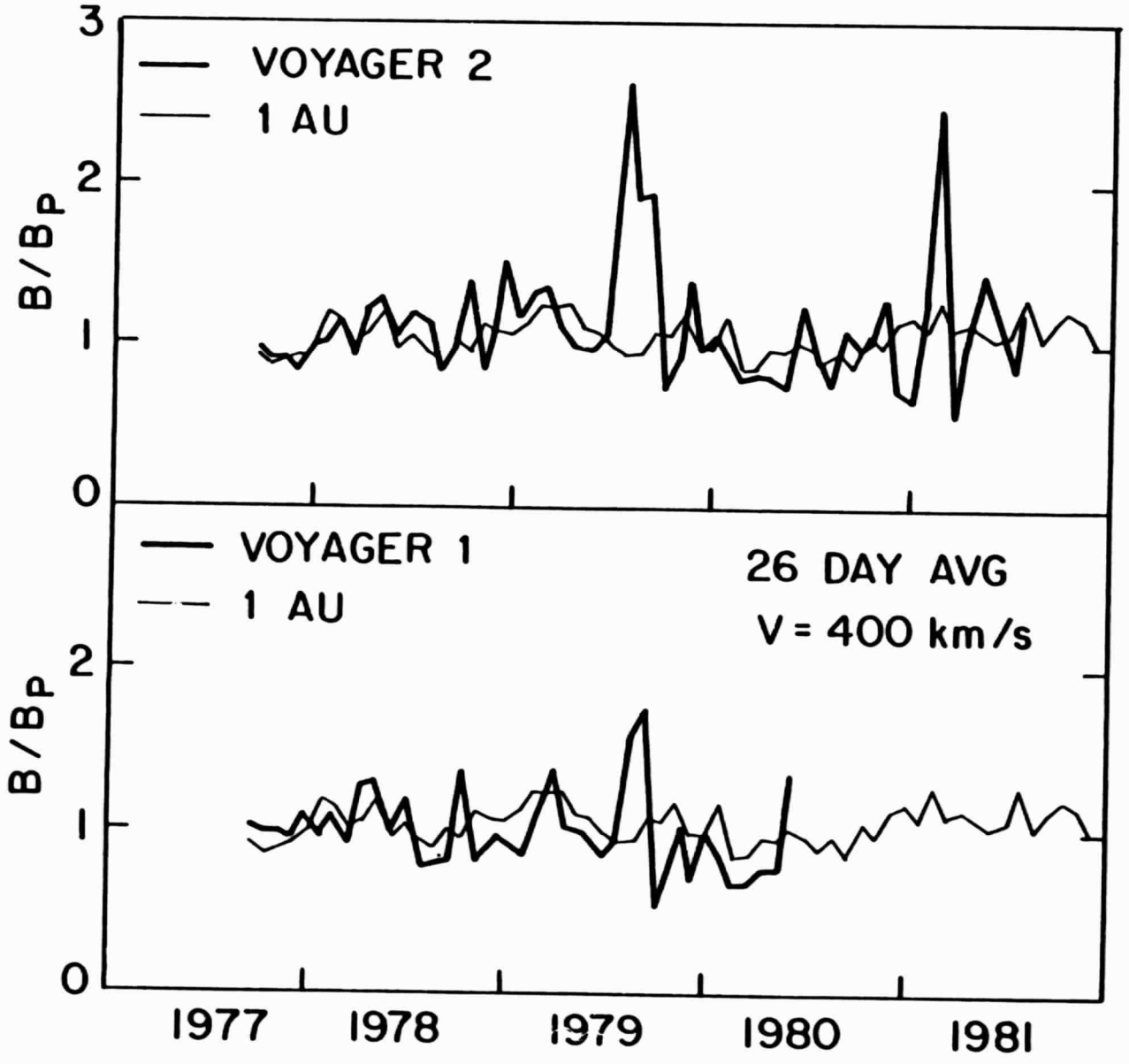
VOYAGER 2
1 AU
B/Bp
3
2
1
0
VOYAGER 1
1 AU
26 DAY AVG
V = 400 km/s
B/Bp
2
1
0
1977
1978
1979
1980
1981

Figure 3

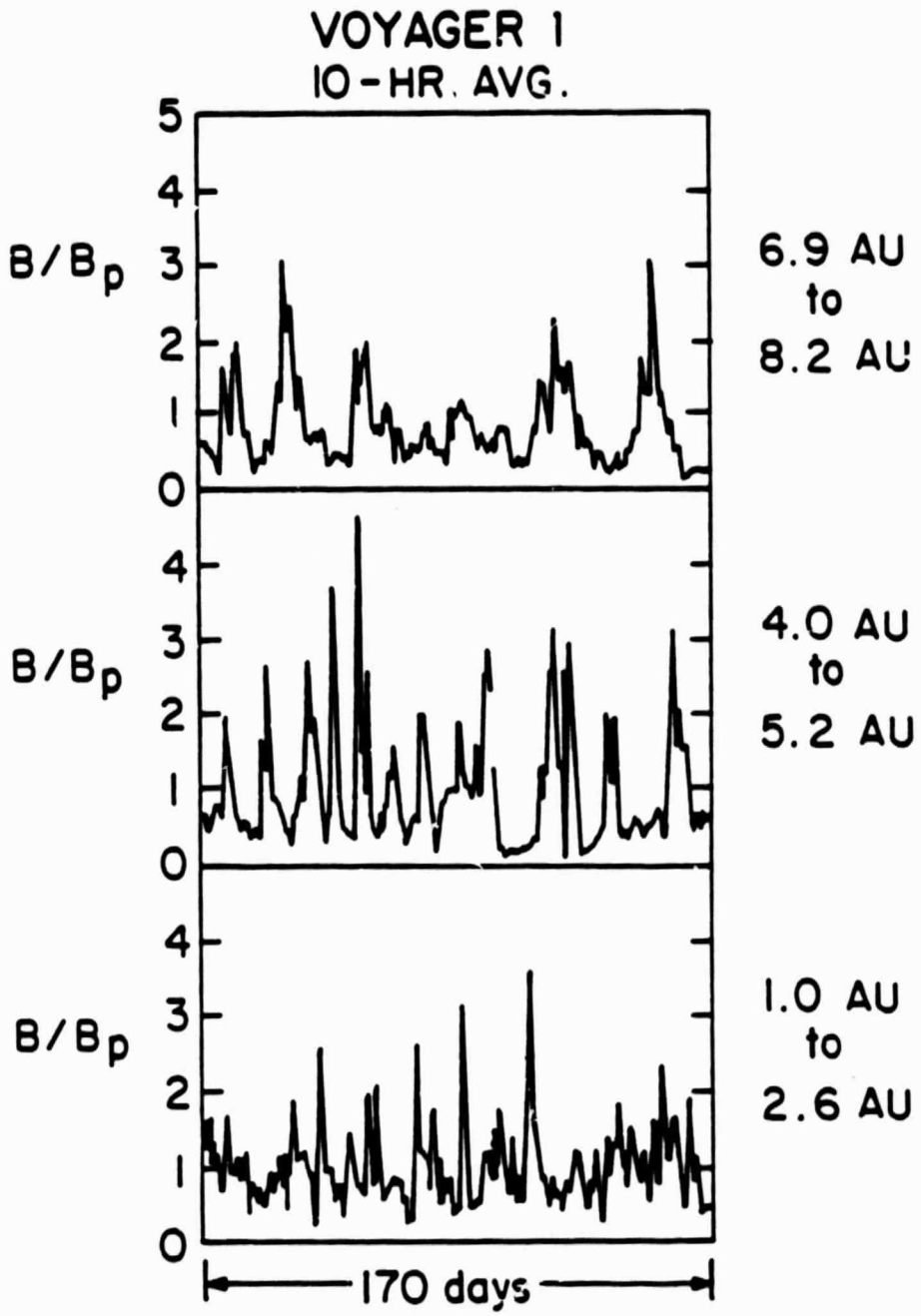
VOYAGER 1
10-HR. AVG.
B/Bp
6.9 AU
to
8.2 AU
4.0 AU
to
5.2 AU
1.0 AU
to
2.6 AU
0
1
2
3
4
5
170 days

Figure 4

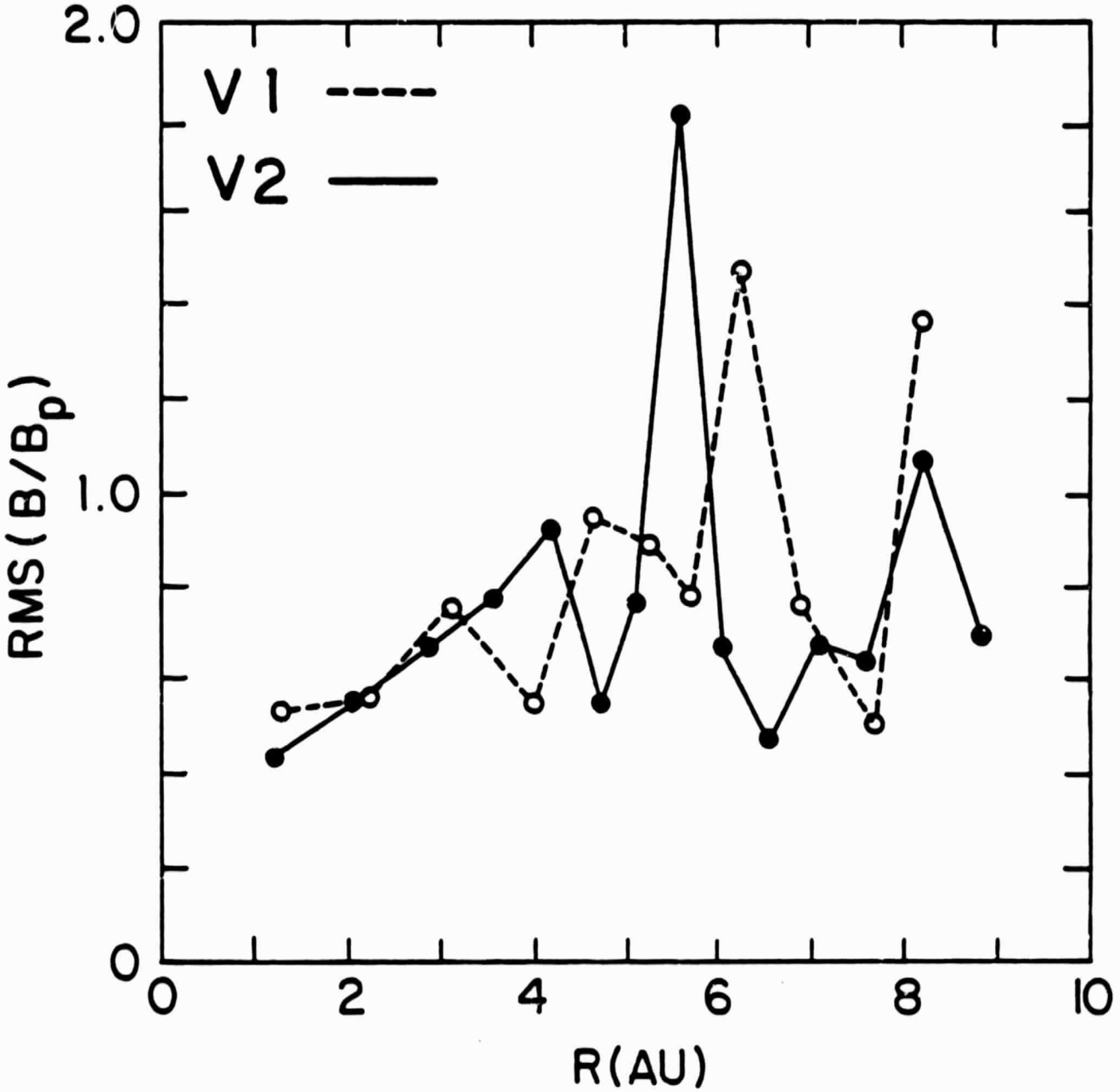

Figure 5

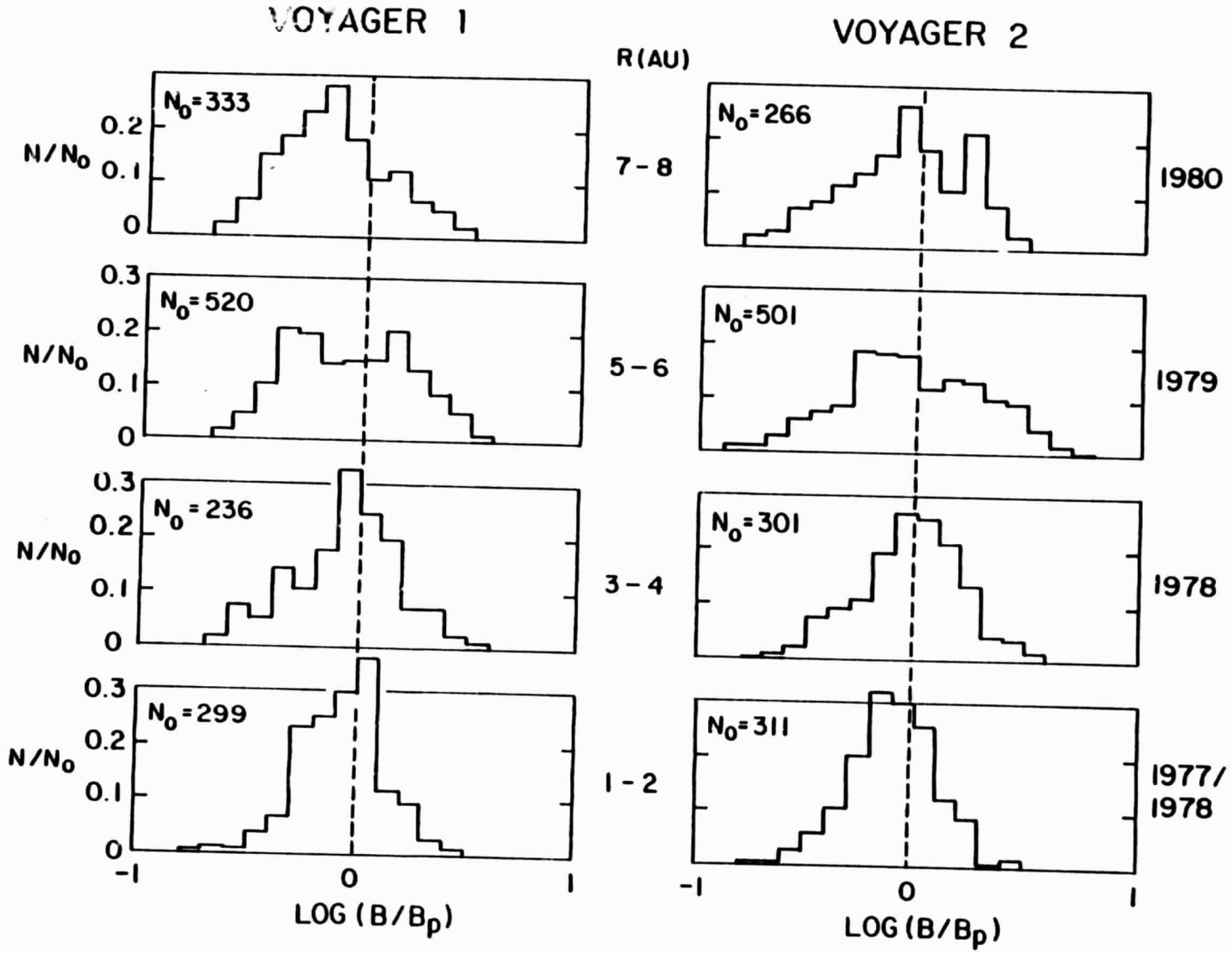
VOYAGER 1
VOYAGER 2
R(AU)
N/N0
N0=333
N0=266
7-8
1980
N0=520
N0=501
5-6
1979
N0=236
N0=301
3-4
1978
N0=299
N0=311
1-2
1977/
1978
0.3
0.2
0.1
0
-1
0
1
LOG (B/Bp)

Figure 6

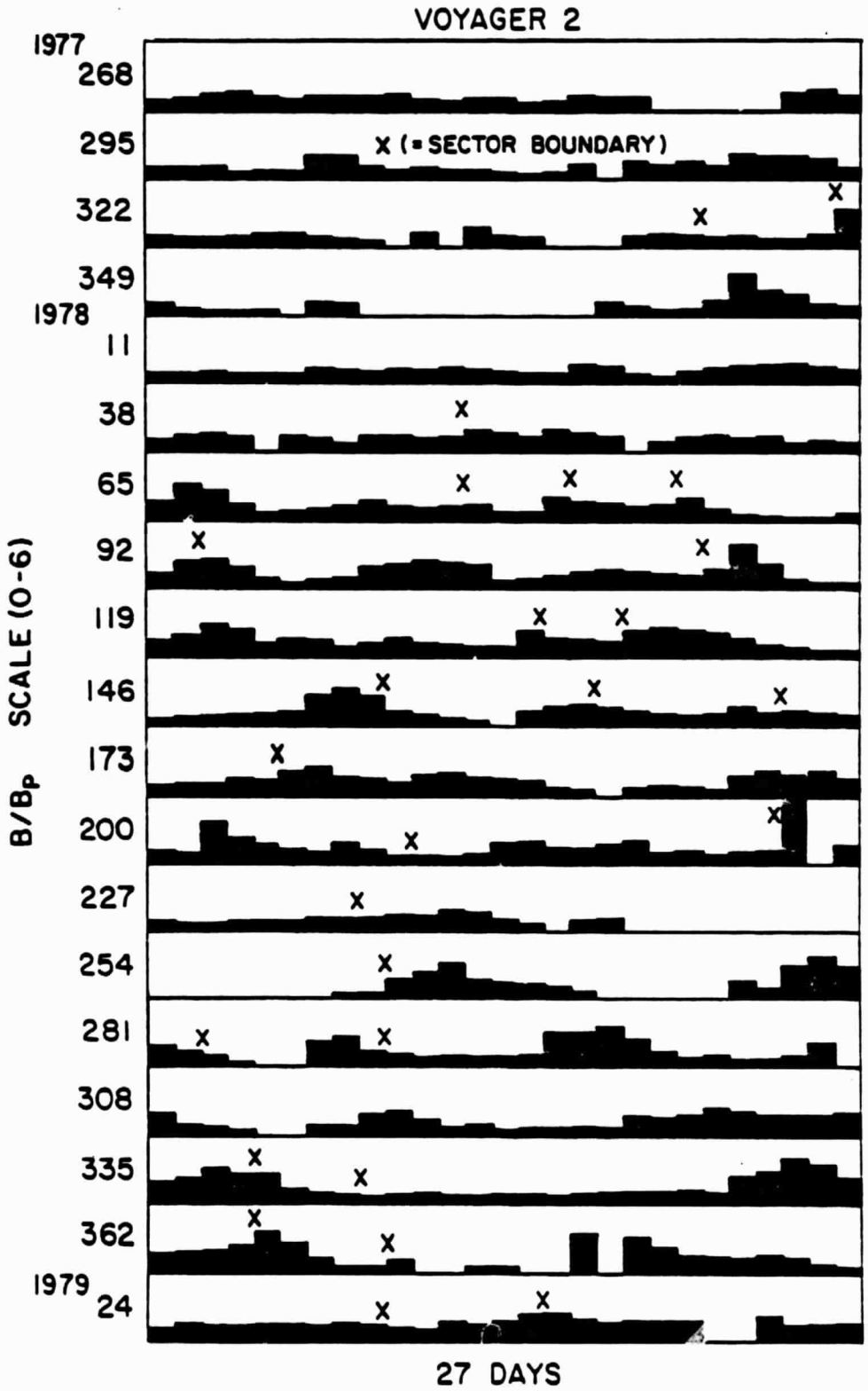

Figure 7

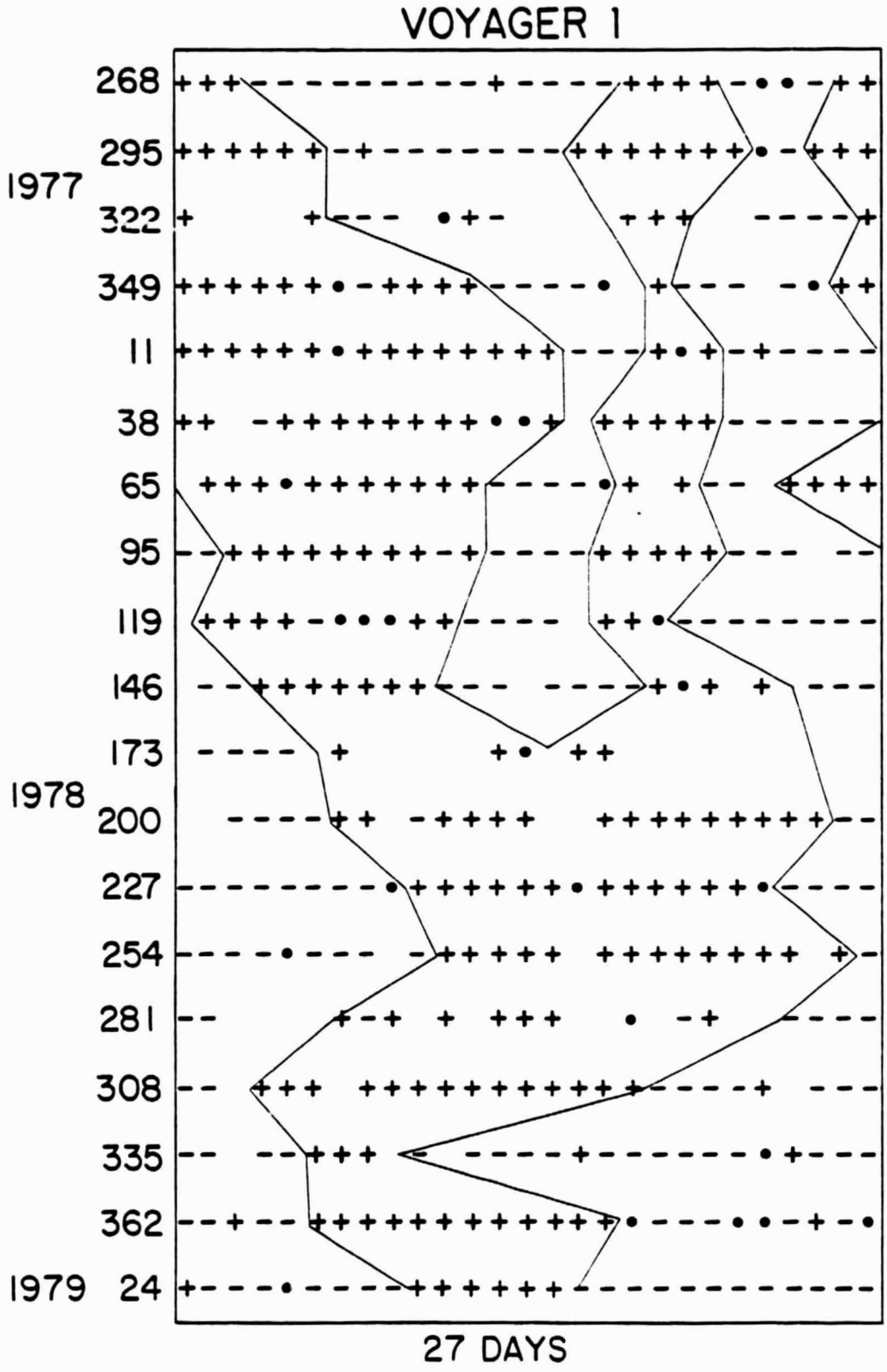

Figure 8

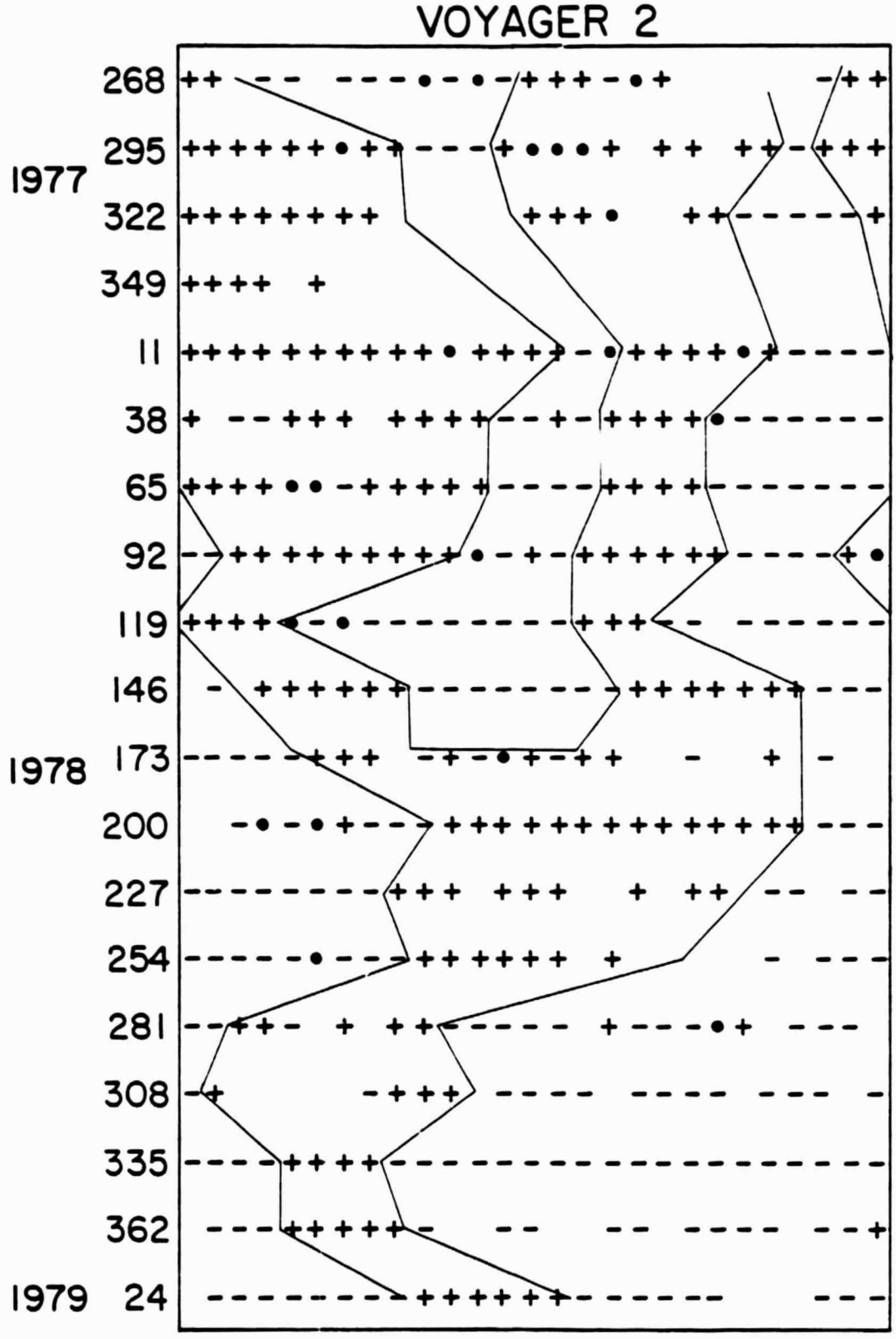
VOYAGER 2
1977
1978
1979
268
295
322
349
11
38
65
92
119
146
173
200
227
254
281
308
335
362
24

Figure 9

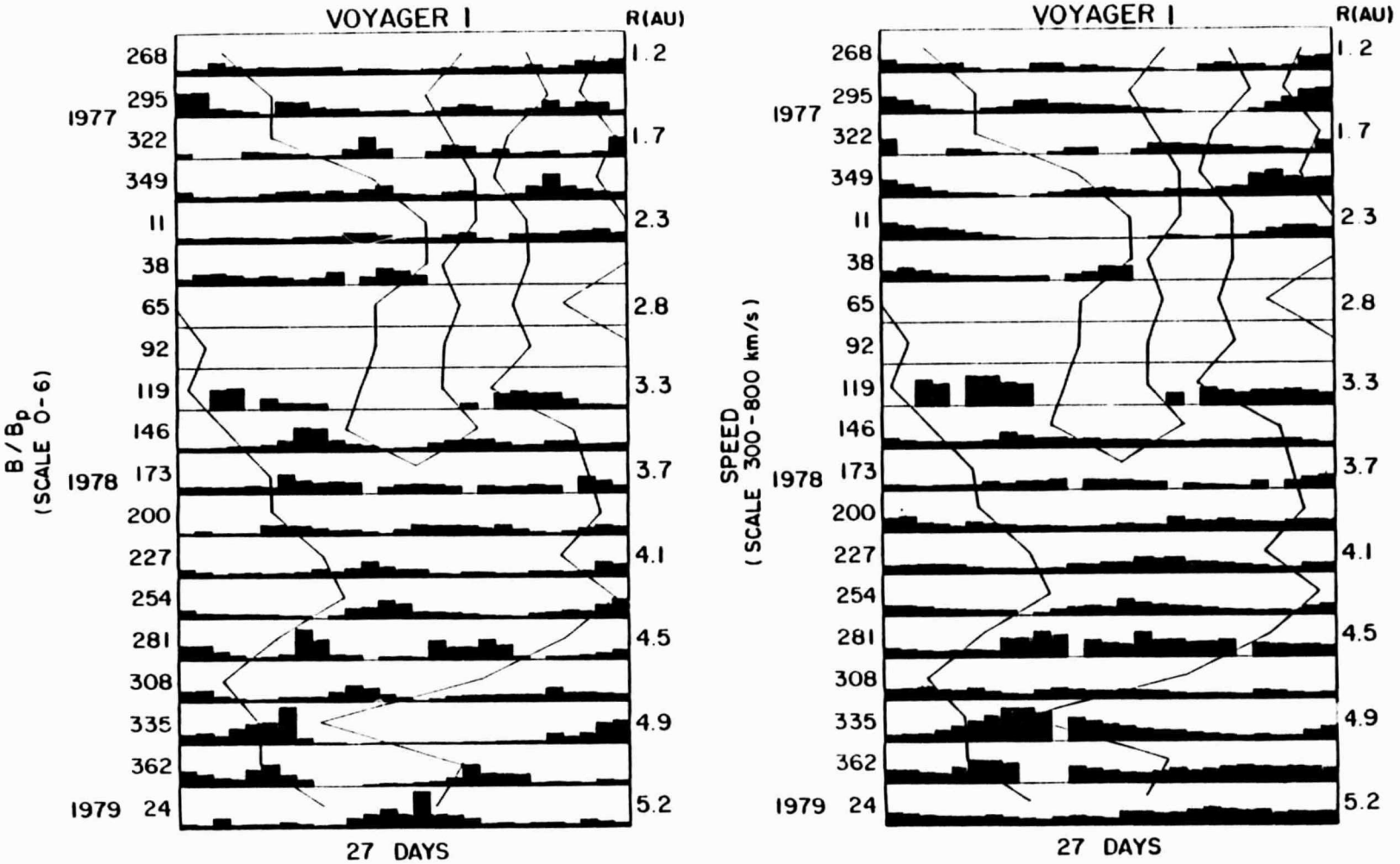

Figure 10

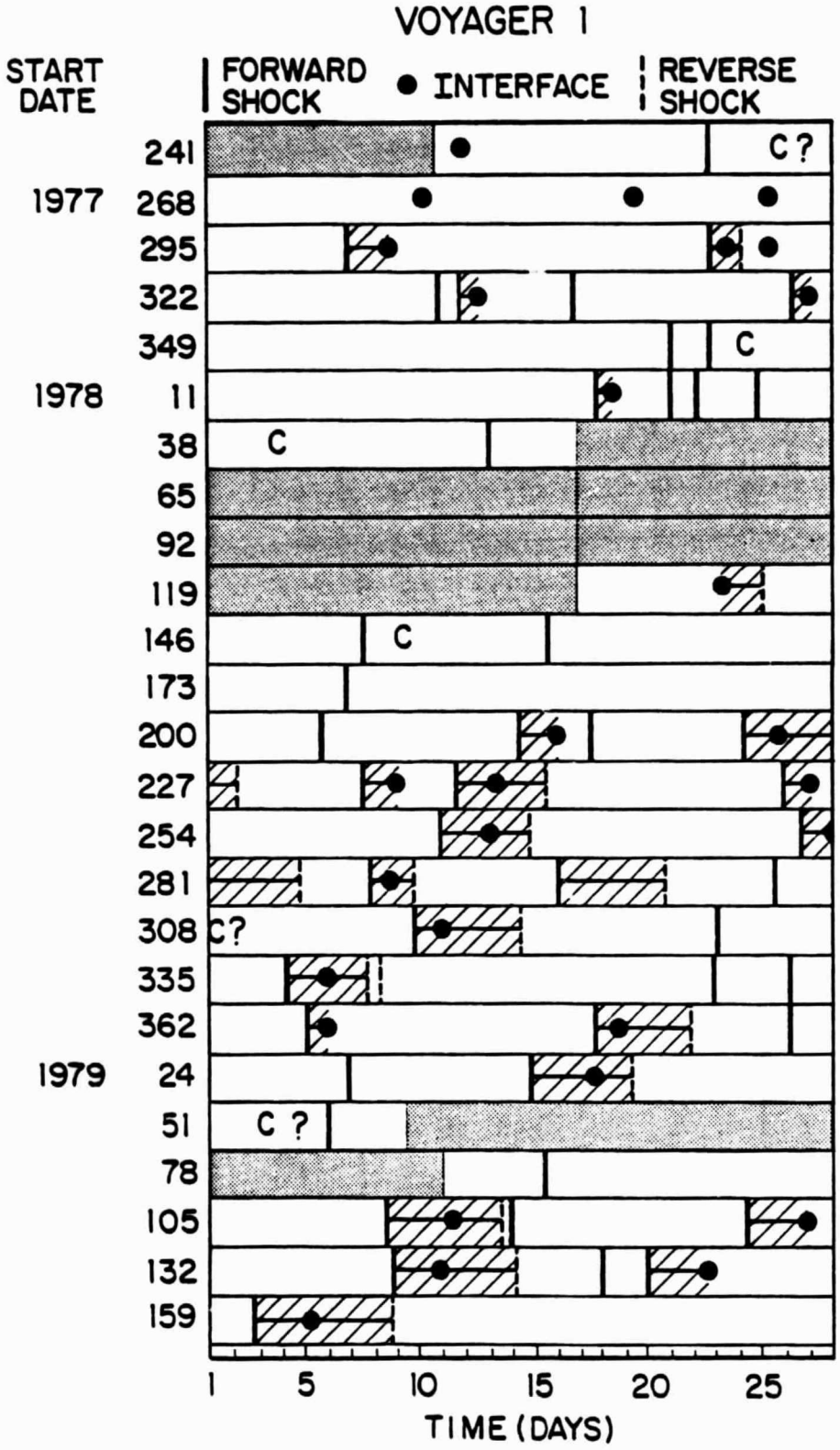
VOYAGER 1
START DATE
FORWARD SHOCK
INTERFACE
REVERSE SHOCK
1977
1978
1979
241
268
295
322
349
11
38
65
92
119
146
173
200
227
254
281
308
335
362
24
51
78
105
132
159
C?
C
C?
C ?
1
5
10
15
20
25
TIME (DAYS)

Figure 11

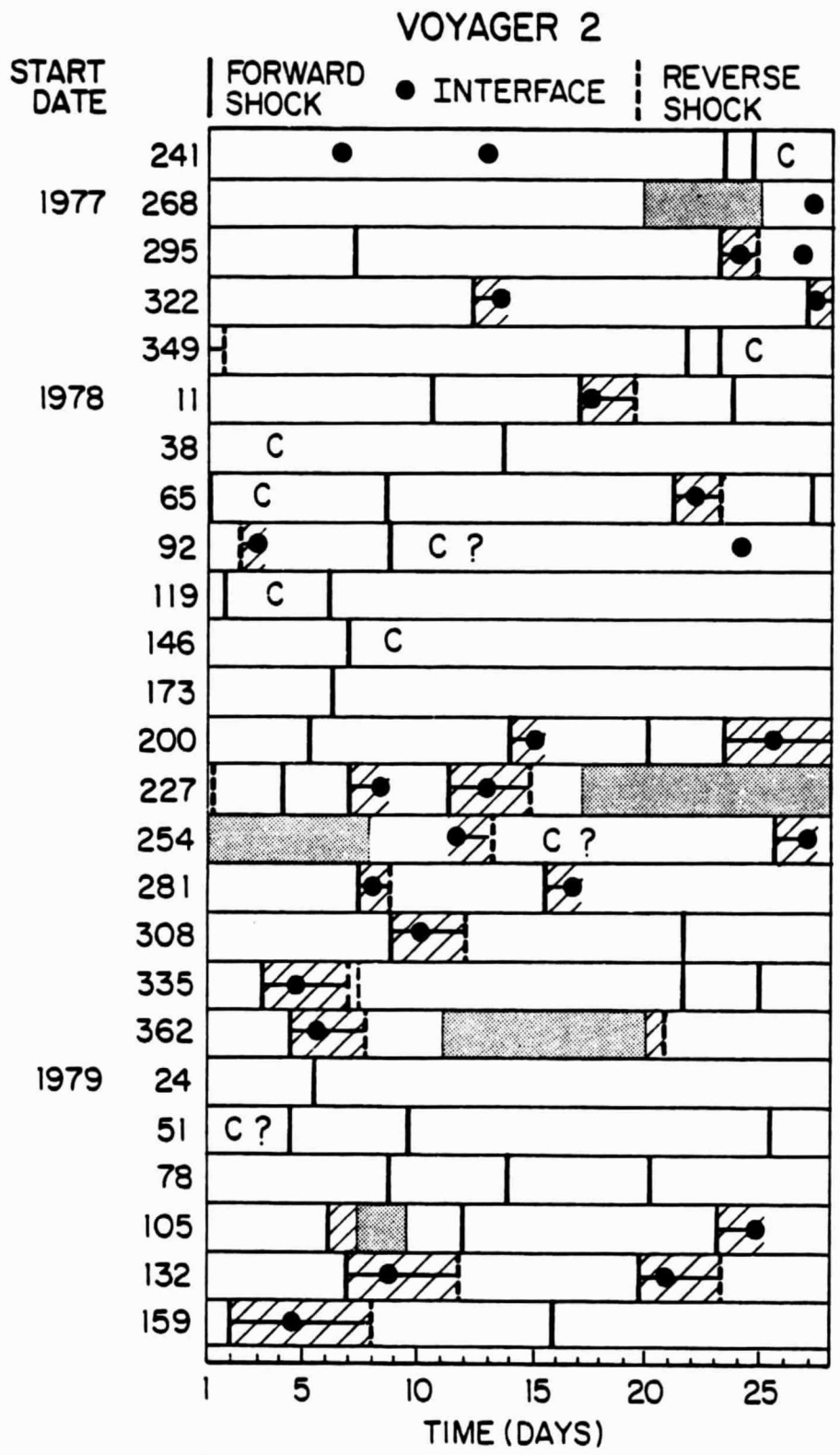

Figure 12

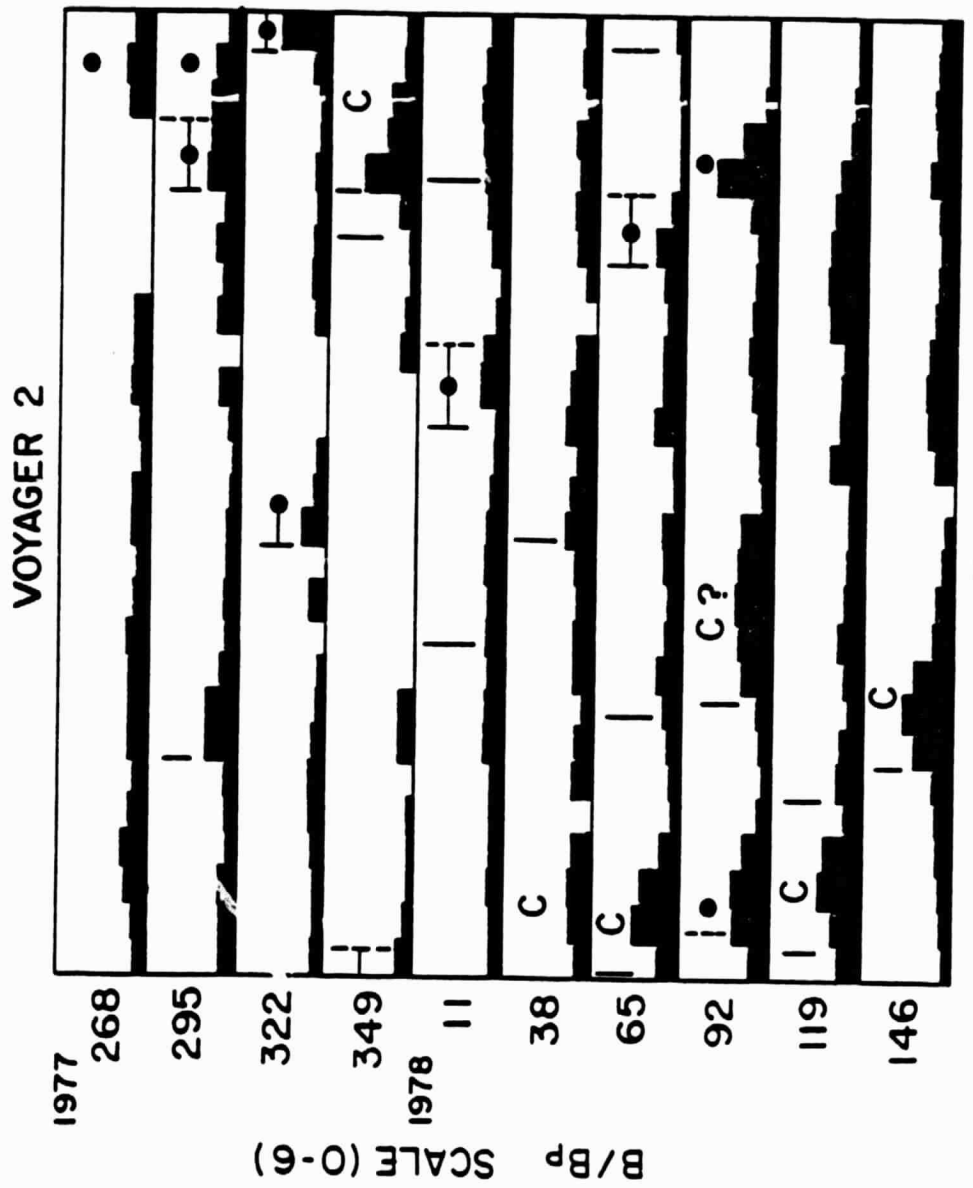

Figure 13a

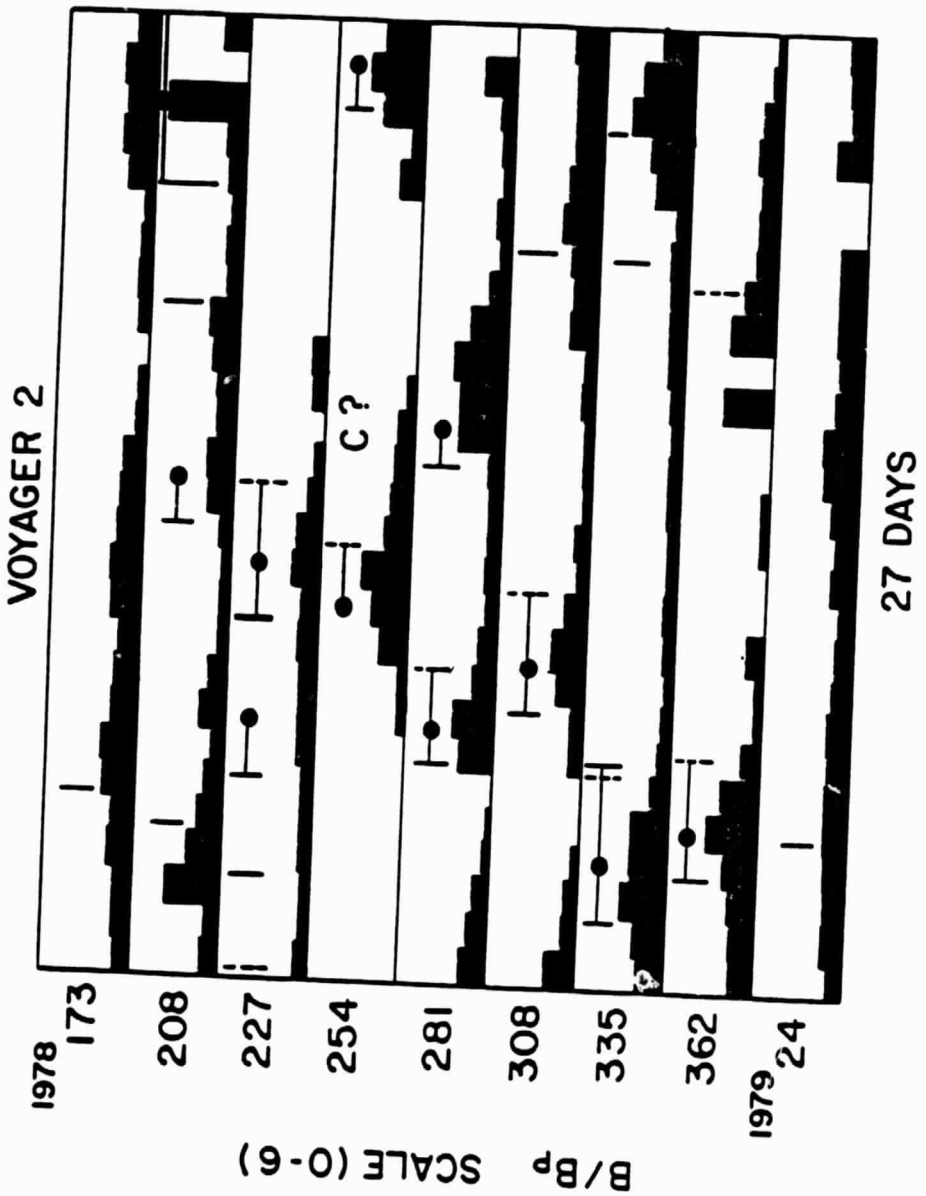

Figure 13b

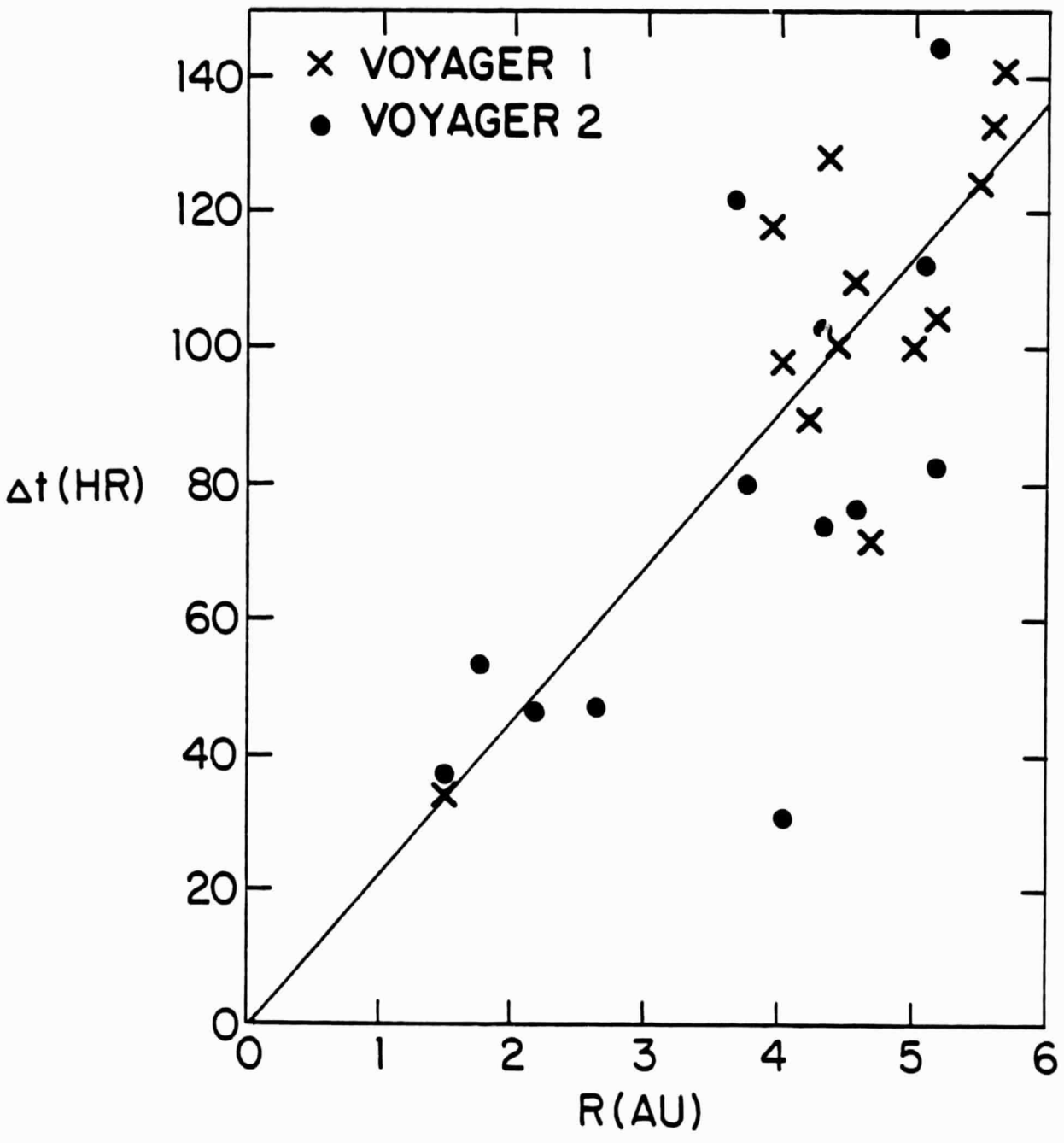

Figure 14

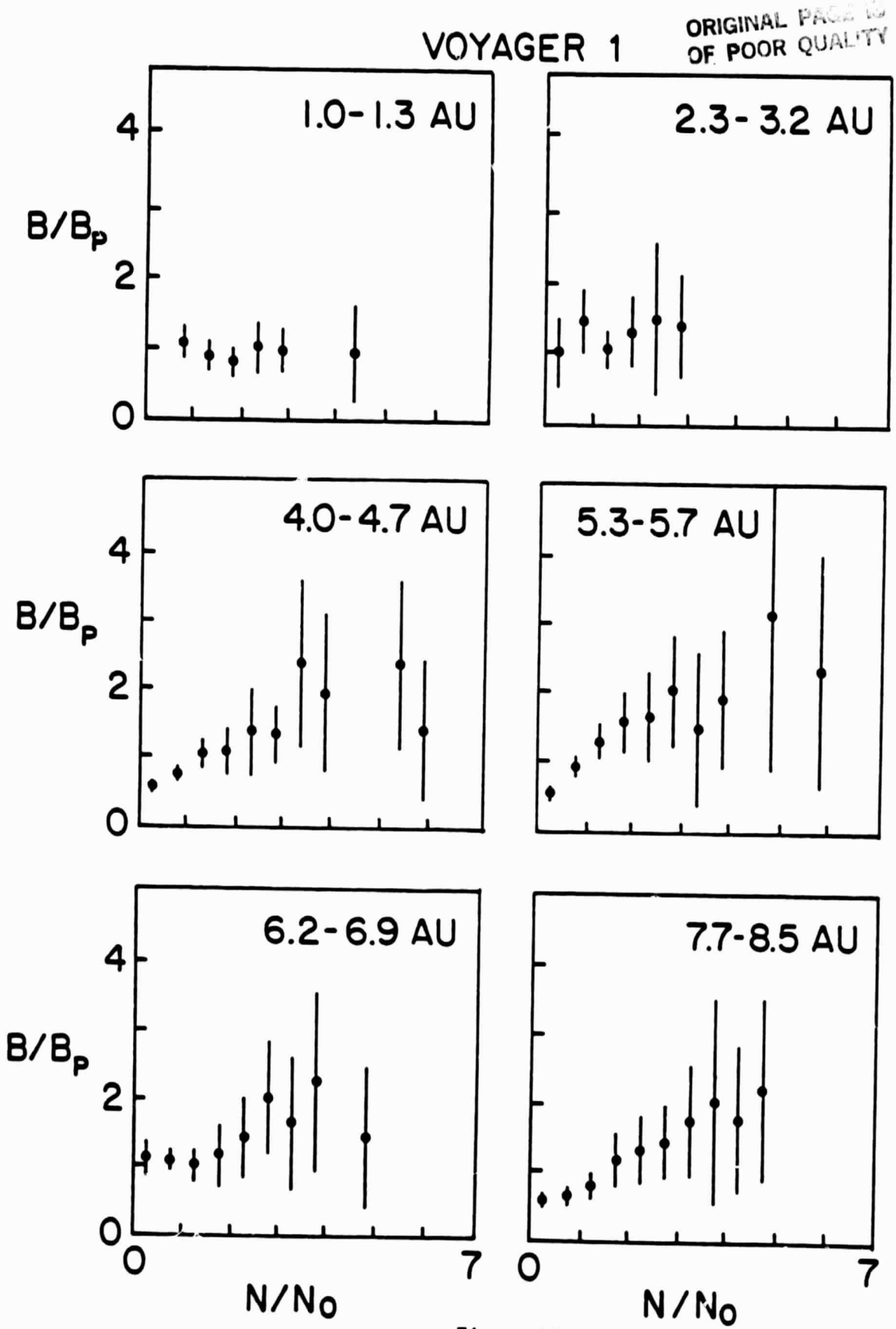

Figure 15